

PAPER

Cite this: *Nanoscale Adv.*, 2021, 3, 240

Inkjet printing of silver nanowires on flexible surfaces and methodologies to improve the conductivity and stability of the printed patterns†

Prathamesh Patil,^{‡ab} Suneha Patil,^{‡a} Prachi Kate^a and Amol A. Kulkarni^{ID} ^{*a}

Silver nanowires (AgNWs) are known to be used for printing on rigid as well as flexible surfaces. Here we have developed a systematic approach for using AgNWs synthesized by the polyol method for printing on flexible surfaces using a simple inkjet printing method. Optimized ink formulation used in this work comprises a mixture of Ag NWs suspended in ethylene glycol directly taken after synthesis and isopropyl alcohol. Using such formulation saves time and loss of material while transferring to other solvents, which is the usual practice. The printed patterns demonstrate high conductivity and stability over many months, which can revolutionize the applications of functional nanomaterials in low-cost printed electronics. The importance of fragmentation of nanowires only to achieve specific aspect ratios, to facilitate easy jetting and to prevent clogging is demonstrated. Varied concentrations (10 mg mL⁻¹ to 50 mg mL⁻¹) of Ag NWs are used in ink formulations in order to print highly conductive patterns (resistance < 50 Ω sq⁻¹) in a minimal number of passes. The same composition was also seen to facilitate simple and time-efficient nano-welding at room temperature, which improves the conductivity and stability of the printed patterns.

Received 19th August 2020
Accepted 4th November 2020

DOI: 10.1039/d0na00684j

rsc.li/nanoscale-advances

Introduction

The development of low cost printed electronic devices will be revolutionized by the ability to print conductive inks made of a wide range of functional nanomaterials in a simple and cost-efficient manner. Conductive ink formulations are typically made by diffusing conductive materials into a solvent and can conduct electricity after printing on an object, thus being a more economical approach to lay down modern conductive tracks. Due to applications in wide-ranging areas including solar photovoltaics,¹ electronic textile and wearable electronics,^{1,2} 3D printed electronics,³ flexible hybrid electronics (FHE), touch screen edge electrodes,^{4,5} automotive defoggers, seat occupancy sensors, seat heaters, *etc.*, ITO replacement (hybrid, direct printing, *etc.*),^{6,7} electronic tattoos,⁸ touch screens for smart phones and tablets,⁵ fillers in high performance conductive adhesives⁹⁻¹¹ and LEDs, LCDs and OLED displays,^{6,12} there is a huge booming consumer market for conducting inks. Furthermore, with the development of electronic printing technology, conductive thin films are widely used in flexible display circuit printing¹³ and to improvise or repair circuits on printed circuit boards as well. Conductive inks

can be printed on flexible surfaces by several methods such as drop casting,¹⁴ spin coating,^{15,16} screen printing,¹⁷ digital printing (inkjet technology),^{3,13,18-23} gravure printing,²⁴ flexography and the roller ball pen method.²⁵ Among all the methods, inkjet has a high utilization of materials on a large area with precision and is a simple and low-cost manufacturing process.

Inkjet printers are the most commonly used type of printers which recreate a digital image by propelling droplets of ink onto paper and plastic substrates. Depending on the utilization of the printing method, inks are often formulated with their distinctive stability and wettability. The composition of conductive ink comprises mainly a metal nanostructure in combination with solvents, capping agents, additives, antioxidants, UV absorbers and adhesion promoters. Functional nanomaterials such as gold nanoparticles, silver nanoparticles and nanowires, graphene, carbon nanotubes, copper nanoparticles, due to their enhanced thermal and electrical properties at the nanoscale and relatively very low quantity needed to achieve the desired performance attracted significant attention for their use in such applications.²¹ Amongst them, a one-dimensional form of silver, *i.e.* silver nanowires (AgNWs) has gained enormous demand because of its very high conductivity (6.30 × 10⁷ S m⁻¹ at 20 °C; highest among all metals) and the high aspect ratio of nanowires helped enable their use in transparent conducting applications as well.^{21,26,27} Various methods have been developed for synthesizing Ag NWs such as the chemical reduction method,²⁸ microwave-assisted synthesis,²⁹ solvothermal method,³⁰ template assisted method³¹ and ultra-violet irradiation method.³² The polyol

^aChem. Eng. & Proc. Dev. Div., CSIR-National Chemical Laboratory, Pune, 411008, India. E-mail: aa.kulkarni@ncl.res.in^bChem. Eng. Dept., National Institute of Technology Calicut, Kozhikode, India

† Electronic supplementary information (ESI) available. See DOI: 10.1039/d0na00684j

‡ Equal contribution.



method is one of the most reproducible methods^{27,33,34} used for the production of silver nanowires. The method involves using a polyol solvent such as ethylene glycol to reduce the precursor Ag^+ ion to Ag^0 to form single crystalline and mono-crystalline particles, which led to subsequent formation of nanowires by selective unidirectional growth. Synthesis of silver nanowires is a highly sensitive process as even a slight variation in the process parameters *viz.* temperature, concentrations (of the reducing agent, substrate an capping agent), the molecular weight of the capping agent, the reaction time, *etc.* can lead to a change in the diameter and aspect ratio (*i.e.* length) of nanowires and in turn affect their end-application.¹³ Silver nanowires with aspect ratios (<500) can be used in conductive ink compositions^{8,26,35} which can be printed on a wide range of rigid and flexible substrates to provide conductive thin films or coatings. External treatment methods such as sintering, laser and microwave techniques are carried out to further increase the conductivity in applications.³⁶ Sintering is a heat treatment technique performed at room as well as high temperatures in order to improve the connection between two nanoparticles or nanowires.^{3,22,23,36,37} There is a need to improve the techniques for increasing the conductivity of the printed metallic networks. Thermal treatment requires precise control of the heating temperature and time as otherwise, the nanomaterial can oxidize or can get damaged on heat sensitive substrates especially plastics.³⁸ Mechanical treatments such as pressing when applied to certain devices, high pressure may destroy some useful structures or the active layer. A simple but effective approach is using capillarity to improve the contact of wire junctions, which can form closely packed structures of nanoparticles that float or are immersed in liquids.³⁹ In view of this we have studied the preparation of inkjet printing inks and developed a simple method to print highly conducting and stable patterns on flexible surfaces using the directly synthesized suspension of AgNWs in EG as it is.

The manuscript is organized as follows: after the Introduction, we have given details of experiments that involve developing formulations using silver nanowires. Further we have demonstrated the utilization of silver nanowires (in the form of conducting inks) for digital printing using easy-to-use inkjet printers. A detailed analysis of the number of passes and effective conductivity of the tracks on a paper is also presented. It was observed that our formulation was suitable for nano-welding at room temperature⁷ by applying moisture to the printed nanostructures, which helps increasing the number of points of contact. Furthermore, we have shown that by coating the surface of the nanowires with an additive polyaniline (PANI), not only the stability of the material is increased, but also a significant decrease in the resistance of the patterns is observed. Finally, we summarize the important findings.

Experimental

Materials

All chemical reagents were purchased from Merck GmbH and used without any further purification. Silver nitrate (AgNO_3 , 99.8%), Ethylene Glycol (EG, 99%), ferric chloride hexahydrate

(anhydrous $\text{FeCl}_3 \cdot 6\text{H}_2\text{O}$), and polyvinylpyrrolidone ((PVP) K90:360000) were used for the synthesis of silver nanowires. The synthesized silver nanowires (in ethylene glycol) were dispersed in isopropyl alcohol (99.7%) according to the optimal ink solvent ratio. For printing purposes, an A4 size paper sheet, PET sheet, commercial printer HP Deskjet Ink Advantage All-in-One Series – K209 were used.

Synthesis procedure for AgNWs

Initially, ~ 0.2 g of PVP was added to 22 mL of preheated Ethylene Glycol (EG) at 100 °C, and a constant stirring speed of 500 rpm, in a round bottom flask heated in an oil bath by means of an IKA C Mag HS7 digital heater. Then, 700 μM chloride solution (in EG) was added to the flask, which was then heated to a reaction temperature of 140 °C, after which AgNO_3 solution (in EG) was added drop-wise to the reaction solution. The reaction was held at constant temperature for two hours and nanowire product solution of glistening silver-grey color was obtained, which was allowed to cool at room temperature. For purification of nanowires, product solution was precipitated using acetone (3 times the AgNW synthesis product) as an anti-solvent and the precipitate, after washing with ethanol was centrifuged at 13 500 rpm for about one minute. The precipitate after centrifugation contained pure silver nanowires, which were further used in ink formulations.

Preparation of AgNW ink

Pure silver nanowires were dispersed in a solution comprising a mixture of isopropyl alcohol and ethylene glycol. Ink samples were prepared on the basis of the weight of the nanowire per mL volume of solution of IPA : EG (85 : 15; volume%). The dispersion consisted of different concentrations of nanowire (10 mg mL^{-1} , 20 mg mL^{-1} , 30 mg mL^{-1} , 40 mg mL^{-1} and 50 mg mL^{-1}) samples with an average nanowire length of 10–13 μm . The prepared ink solutions (Fig. 1) were sonicated (to reduce the size of nanowires) for different intervals of time to optimize the length of nanowires so as to prevent clogging and allow unhindered passage of the sample through the nozzle of the cartridge.

Printing set up

Commercially available printer HP Deskjet Ink Advantage All-in-One Series – K209 was used for printing the nanowire suspensions. This printer has a HP Thermal Inkjet head with 336 nozzles and each nozzle is of size 10 μm (diameter), and each



Fig. 1 AgNW ink sample of IPA : EG in a ratio of 85 : 15 with the AgNW concentration ranging from 10 mg mL^{-1} , 20 mg mL^{-1} , 30 mg mL^{-1} , 40 mg mL^{-1} to 50 mg mL^{-1} (left to right).

droplet volume is of the order of 2.5 picoliters. The printer consists of two cartridges, one in black and the other one in color. More details of the cartridge parameters are given in ESI Table 1.† The prints were taken on only single cartridge mode (black) (ESI Fig. 1† shows the image of the black cartridge used for printing). Parameters for the printing of silver nanowire ink such as print quality were set as 'best' and color options to 'print in grey scale' with 'black ink only'. After making a few drawings, various prints of line patterns (length 10 cm and widths of 2, 4, 6, 8, 10 mm), squares, circles, helix and circuit patterns were taken on A4 sheets using the inkjet printer.

Sintering and electrical measurements

Heat treatment. Ink samples were spin coated on the surface of a glass slide (1.2 cm × 1.2 cm) as shown in ESI Fig. 2.† A drop of 15 μL volume was coated on the glass slide at a spinning speed of 1000 rpm for 60 s. After coating the ink, the substrate was allowed to dry to remove solvent. It was then further heated at different temperatures *viz.* 140 °C, 175 °C, 210 °C, 225 °C, 250 °C, 275 °C and 300 °C for various time scales to track the changes in the electrical conductivity as well as the morphology. An MECO 603 multimeter was used to check resistance.

Cold nano-welding. The spin-coated sample was exposed to water vapours using a water evaporator for about 1 minute in order to condense the water droplets on the coated nanowire patterns. The samples are then subjected to drying at room temperature.

Results and discussion

Optimization of the nanowire morphology by sonication

Length of the nanowire. The FE-SEM images of the as-synthesized AgNWs were analysed for the length and diameter in ImageJ software. The average diameter of the AgNWs was found to be 60 ± 2 nm and average length was in the range of 10–15 μm. The synthesized nanowires were relatively long to pass through the cartridge nozzle of diameter 10 μm, since it is well-known that printing of nanomaterials generally works best when the length dimension of the nanoobject is less than $a/50$ (where 'a' is the nozzle diameter). However, this criterion might not be satisfactory for nanowires due to the possibility of flow-induced alignment, as the wires passed through the nozzles might clog them. Several attempts to flow the nanowire suspension through the nozzles were unsuccessful as within a few seconds the nozzles would get clogged. To optimize the length of the nanowire for smooth passage through the nozzle, AgNWs were sonicated for different time intervals of 30 minutes, 1 hour, 2 hours and 3 hours.⁴⁰ From the characterization images in Fig. 2, it is observed that after 3 hours of sonication, the nanowire length is reduced to 1.18 μm. Trials showed that, even though the length of these wires was larger than $a/50$, they could be successfully ink jetted after sonication for 2 hours. Table 1 illustrates the printing results with a change in the average length and diameter of AgNWs, when ink samples were sonicated. It was observed that the diameter of AgNWs remained unaffected and the prints of samples

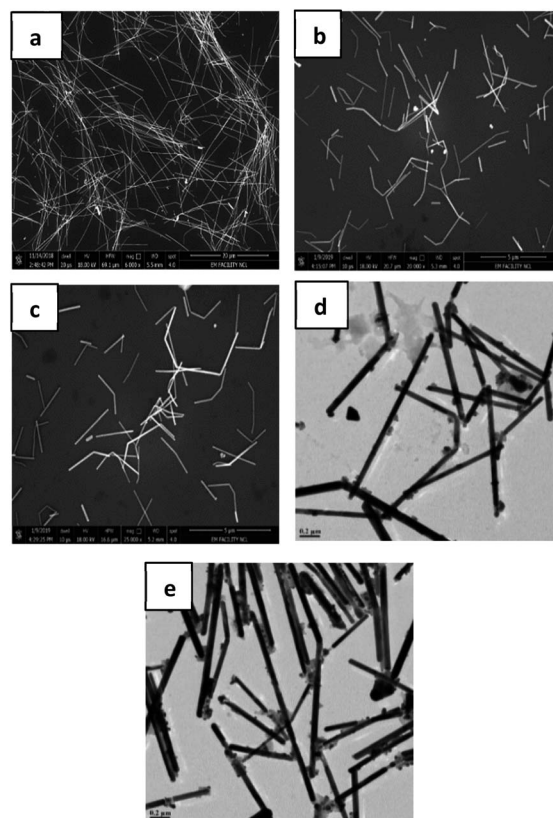


Fig. 2 SEM images of AgNWs after sonication for (a) 0 min [50–100 μm], (b) 30 minutes [2–10 μm], and (c) 1 hour [1–5 μm]; TEM images of AgNWs after sonication for (d) 2 hours [0.8–1.8 μm], and (e) 3 hours [0.6–1.2 μm].

Table 1 Effect of the sonication time on scission of the nanowire length

Sonication time	Average length of the nanowire (μm)	Average diameter of the nanowire (nm)	Result
No sonication	10–13	61	Not jettable
30 minutes	3.77	61	Cartridge gets clogged in the first print
1 hour	2.81	61	Cartridge gets clogged after 5–6 prints
2 hours	1.72	61	Optimum AgNW length for printing with no break in the conducting tracks
3 hours	1.18	61	No clogging of the cartridge. Very short AgNWs result in lower conductivity when compared to sonication of 2 hours

sonicated for 2 hours (AgNWs length ~ 1.7 μm) gave better conductivity than the ones sonicated for larger intervals (3 hours, 1.18 μm). Hence, nanowires having a length of 1.7 μm were considered as the optimized length for smooth printing without clogging the nozzle and had better conductivity.

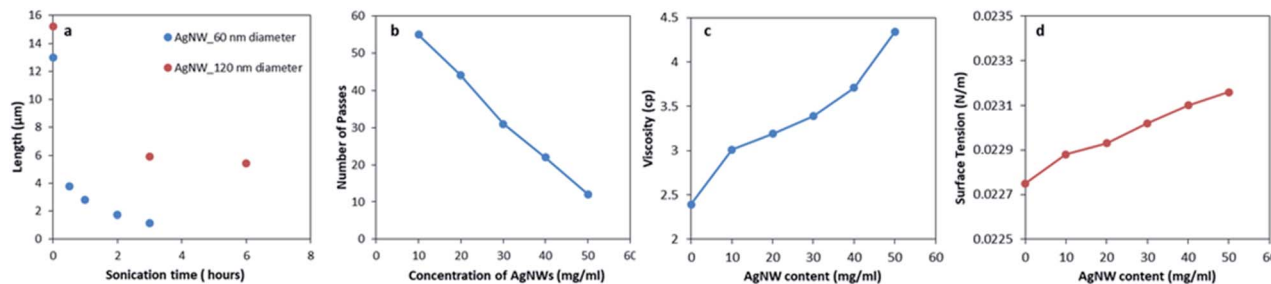


Fig. 3 (a) Effect of the sonication time on fragmentation of silver nanowires; (b) number of printing passes required with respect to the concentration of AgNWs; (c) and (d) viscosity and surface tension variation of the ink sample respectively with respect to the concentration of AgNWs in the ink sample.

Diameter of the nanowire. In order to check the applicability of AgNWs with lower aspect ratios (100–150), ink formulations of AgNWs (diameter ~ 121 nm, length ~ 15 μm) (ESI Fig. 3a†) were prepared. Samples were sonicated for 3 hours and 6 hours, but the optimized length was not obtained even after sonication for as long as 6 hours (ESI Fig. 3b†) and the final reduced AgNW length was 5.4 μm . These AgNWs were capable of clogging the nozzles. Following Hook's law, large diameter wires would need energy proportional to their cross-sectional area and Young's modulus of the material. They also need more time under sonication to fragment them in smaller fragments.

A comparison of the sonication effect on the length of two nanowire diameters (>100 nm and ~ 60 nm) is plotted in Fig. 3a. Since, <2 μm (optimized length for NWs) is attained only for AgNWs with an average diameter of 60 nm or below, these NWs only can be considered for formulating conducting ink solutions for printing purpose.

Optimization of the concentration of nanowires in ink

According to most of the literature, 10–15 numbers of passes are an acceptable range of repeated passes to make a pattern conductive. However, in general, it is necessary to minimize the number of passes and yet obtain a conducting track. Here we have obtained optimal numbers of passes by increasing the concentration of the nanowire concentration in the ink from 10 to 50 mg mL^{-1} . With increase in the AgNW concentration, the

numbers of passes required to make the pattern conductive decreased, which is plotted in Fig. 3b. For 50 mg mL^{-1} concentration, the numbers of passes to obtain a continuous conducting track was 12, which agrees with the literature data.

The two most important properties of ink are viscosity (resistance to flow) and surface tension as they decide the ease of detachment from the nozzle and also spreading on the surface. The viscosity and surface tension of the samples were measured and are shown in Fig. 3c and d respectively. The values of both viscosity and surface tension were seen to increase with the silver concentration and are in agreement with data in the literature.¹⁸ For the weight concentration of mere 5% silver nanowires (50 mg mL^{-1}), the ink sample has a viscosity of ~ 4.4 cP, which is in the acceptable range of commercial inkjet printing inks (1–30 cP).^{18,20} The relatively lower surface tension (~ 23 mN m^{-1} when compared to 27–35 mN m^{-1} in commercially available ink¹⁸) can be increased by increasing the wt% of Ag in the sample. However, in our case, using 5 wt% concentration does not affect printing significantly because after the addition of the additive the surface tension of the sample measures in the permissible range (~ 30 mN m^{-1}). Utilization of silver nanowires in inkjet inks is beneficial because these nanowire-based inks perform well in printing even at very low concentrations of silver (5 wt%) as compared to commercially available AgNP based inks with much higher Ag concentrations (19–21%).^{22,23} Inkjet printing is more appropriate for AgNW inks as the method works well for such low viscosity inks.

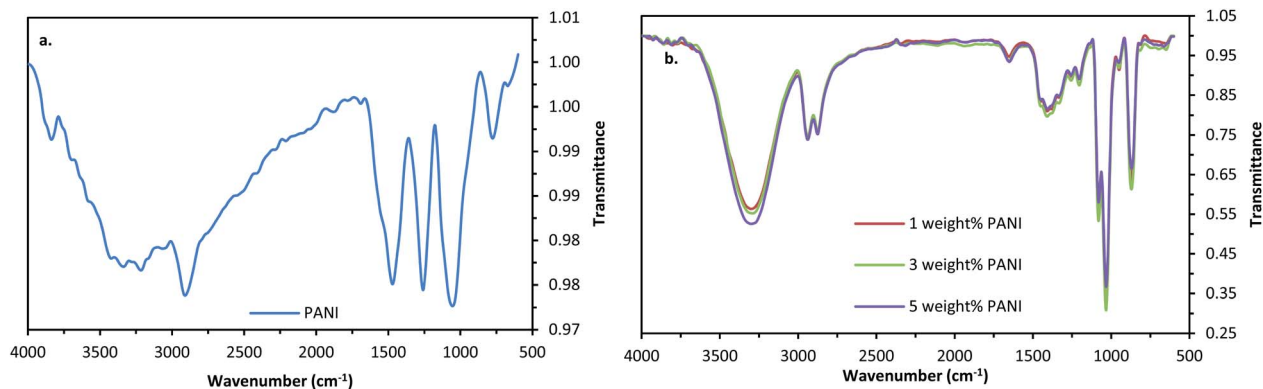


Fig. 4 Infrared spectra of (a) PANI; (b) 1 wt%, 3 wt% and 5 wt% PANI–AgNW conductive ink.

Stability of nanowires

Additives are key factors in the production of high-performance conductive inks, and also should be compatible with the nano materials and substrates used. Polyaniline (PANI), polythiophene, and polypyrrole (PPy) can be used as stabilizing agents as they are conductive polymers, but among all conductive polymers PANI has the highest conductivity because of the C–N extended conjugation while all other polymers have a C–C single bond. PANI was chosen as the stabilizing agent due to its higher conductivity and stronger antioxidant properties in this work. Chemical synthesis of PANI requires three reactants: aniline, an acidic medium and an oxidant. Hydrochloric acid (HCl) and sulphuric acid (H₂SO₄) are the most common acids used for synthesis. As for oxidants, it is recommended to use ammonium persulfate ((NH₄)₂S₂O₈), potassium dichromate (K₂Cr₂O₇), cerium sulphate (Ce(SO₄)₂), sodium vanadate (NaVO₃), potassium ferricyanide (K₃(Fe(CN)₆)), potassium iodate (KIO₃), and hydrogen peroxide (H₂O₂).¹¹ We have used the most common chemical oxidation method in which the oxidant to aniline ratio is kept as 1 : 1 in order to obtain high conductivity. Synthesis is performed by mixing 0.29 mol L⁻¹ aqueous HCl solution with a mixture of 0.28 mol L⁻¹ aniline and 0.28 mol L⁻¹ ammonium persulfate and stirred at 2 rpm.³⁷ The reaction temperature was maintained at 0–2 °C for 2 hours. The precipitate obtained was removed by filtration and washed with HCl and vacuum-dried for 1 hour. The prepared PANI powder was then added to the ink sample in various weight percentages such as 1%, 3% and 5% of the weight of the AgNWs in ink formulation. The above figures represent the FTIR spectra of polyaniline and polyaniline–silver nanowire composite ink. Fig. 4a presents the FTIR spectra of PANI in which characteristic peaks of PANI were observed at 757 cm⁻¹ (*m*-disubstituted Ar C–H bend), 1688 cm⁻¹ (C=C, leucoemeraldine), 1250 cm⁻¹ (C–N stretching vibrations, CAr–N) and 3333 cm⁻¹ (N–H stretching). The strong peaks at 2891 cm⁻¹ are assigned to the asymmetric and symmetric stretching vibration modes of methyl groups.⁴⁰ The characteristic absorption bands at 1037 cm⁻¹ correspond to the (C=N) stretching vibration,⁴¹ whereas the sharp peak at 1457 cm⁻¹ corresponds to the stretching mode of the N–B–N group of protonated PANI.⁴² The peak at 3834 cm⁻¹ is because of the N–H stretching vibration of the amino group of polyaniline.⁴³

Fig. 4b presents the FTIR spectra of the 1 wt%, 3 wt% and 5 wt% PANI–AgNW conductive ink respectively. It is observed that, even though the wt% of PANI in the ink formulation is changed from 1 wt% to 5 wt%, the FTIR spectra remain unchanged. The majority of the above listed characteristic PANI peaks could be observed in the PANI/Ag spectrum with some overlapping and intensity changes (Fig. 4b). From the comparison between PANI FTIR spectra and the rest all FTIR spectra, it can be seen that 3333 cm⁻¹ (N–H stretching) and 2891 cm⁻¹ (C–H stretching) appear as sharp peaks, and 757 cm⁻¹ (*m*-disubstituted Ar C–H bend) has shifted to 863 cm⁻¹. On the other hand 1250 cm⁻¹ (C–N stretching vibrations, CAr–N), and 1037 cm⁻¹ (C=N stretching vibration) were shifted to 1050 cm⁻¹ and 1028 cm⁻¹ respectively. This could happen due

to a change in the stretching frequency (which only depends on the force and reduced mass) and can be obtained as $\gamma = 1/(2\pi C)\sqrt{(k/\mu)}$, where γ is the stretching frequency, C is the speed of light, k is the force constant, and μ = reduced mass. During doping of silver nanowires with PANI, the reduced mass remains unchanged and the stretching frequency could vary depending on the force constant. A change in charge transfer leads to a change in the force constant. Thus, the AgNW surface gets coated by PANI through the interaction between silver and the C–N bond of PANI.

The prepared sample was spin coated on the glass substrate which shows a far-reaching difference in the conductivity of the coated sample. The sample without the PANI content showed a resistance of about 584 Ω □⁻¹, when coated on a glass substrate at 1000 rpm for 60 s. On the other hand under the same spin coating conditions, ink samples with 1 wt%, 3 wt% and 5 wt% PANI content show low average resistances of 62 Ω □⁻¹, 55 Ω □⁻¹ and 47.5 Ω □⁻¹ respectively. It was observed that resistance reduced by ~90% of its initial value after the addition of PANI, and the resistance remains more or less the same, irrespective of the PANI weight percentage. This implies that even a small quantity (1 wt% PANI or lower) is enough to coat the whole surface of silver nanowires to reduce the average resistance to <60 Ω □⁻¹.

Sintering of nanowires

In order to achieve a highly conductive pattern, sintering of printed nanowires is required. The most common technique for

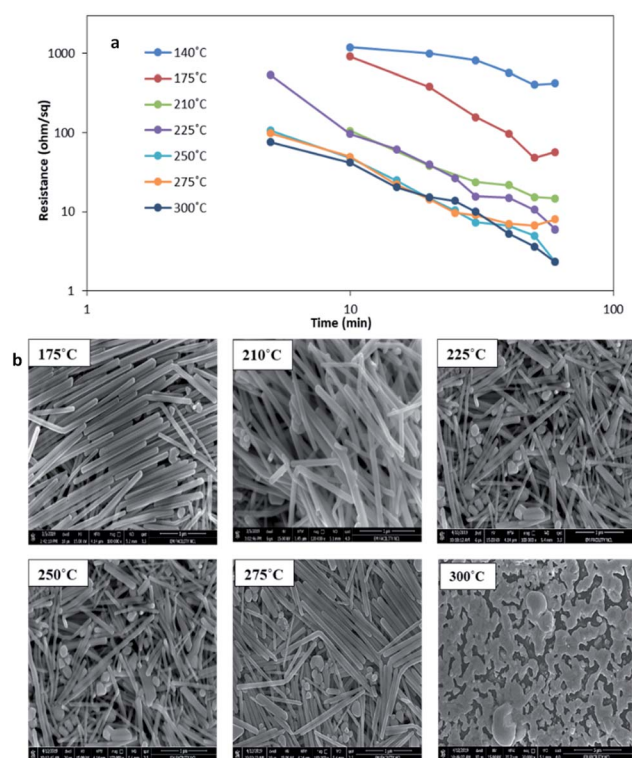


Fig. 5 (a) Electrical resistance as a function of temperature and time and (b) SEM images of silver nanowires after thermal sintering treatment at different temperatures.

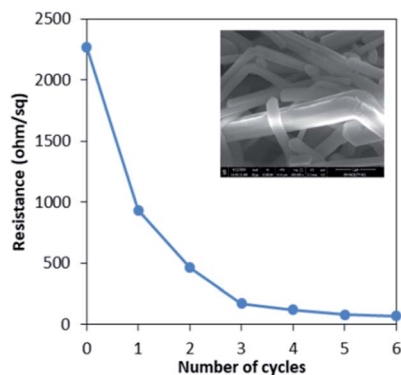


Fig. 6 Electrical resistance after moisture treatment and the inset image showing the NW morphology after moisture treatment.

sintering the nanowires is by conventional heating in an oven or on a hot plate, which requires high temperature as well as long sintering times.²³ Also, there is a possibility of some temperature sensitive substrates getting deformed at high temperatures, thereby leading to oxidation of nanowires in short periods of time. The sintering process usually consists of 2 stages. In the first stage, thermal decomposition and removing of the surfactant (capping agent) are the dominating phenomena. In this stage the high resistance of the printing structure remains stable, because nanowires are separated by organic layers and do not touch each other. In the second stage, the protective layer is removed so that nanoparticles would form at the metallic contact and hence, the diffusion and recrystallization phenomena play the dominating role.²² At the beginning of the second stage, resistance drops significantly due to formation of many chemical paths between the nanoparticles. In this work, we have opted for another sintering method also known as the moisture treatment method. Here, the coated sample was subjected to water vapour for 1 minute, so that vapour condenses and gets trapped at the contact of the nanowires and due to the

capillary force action, the nanowires on the top bend at the contact point after drying.⁸

Effect of sintering on electrical measurements

Conventional heating in a muffle furnace. In consideration of increasing the conductivity of the patterns, the spin coated samples were heat treated in a muffle furnace and the electrical resistance of the samples was then tested. AgNW formulation was spin coated on glass instead of paper as we aimed to study the effect of thermal heating on conductivity and resistivity in a wide temperature range of 140 °C to 300 °C.

The images of AgNW spin coated samples for the surface morphology after undergoing heat treatment at different temperatures for 60 min each are shown in Fig. 5b. A visible effect of sintering on the AgNW samples is seen from the images at temperatures > 175 °C, which instigates the increase in contact between the nanowires and is further confirmed by a decrease in electrical resistance at higher temperatures which is plotted in Fig. 5a as a function of temperature and time. At higher temperatures, the nanowires start melting into nanoparticles, which was due to the evaporation of solvents, thus increasing the interaction between the nanowires and resulting in a significant drop in the resistance. Very high resistances initially are a result of fragmented nanowires. A sudden drop in resistance was observed with the first 10 minutes of heat treatment for the temperature range of 175–300 °C. The resistance continued to drop steadily until 1 hour. In case of lower temperatures such as 140 °C; the resistance of the sample was 403 $\Omega \text{ sq}^{-1}$ by the end of 1 hour of heat treatment (a drop by ~725% in the initial value of 2900 $\Omega \text{ sq}^{-1}$), whereas, for higher temperatures such as above 300 °C, there was a substantial drop in the initial readings to reach as low as ~3 $\Omega \text{ sq}^{-1}$ by 1 hour. It is clear from Fig. 6 that very low resistances (<15 $\Omega \text{ sq}^{-1}$) could be achieved only by treating the samples at temperatures above 200 °C. Moreover, the conductivity of the sample could be influenced by altering the temperature and time of heat

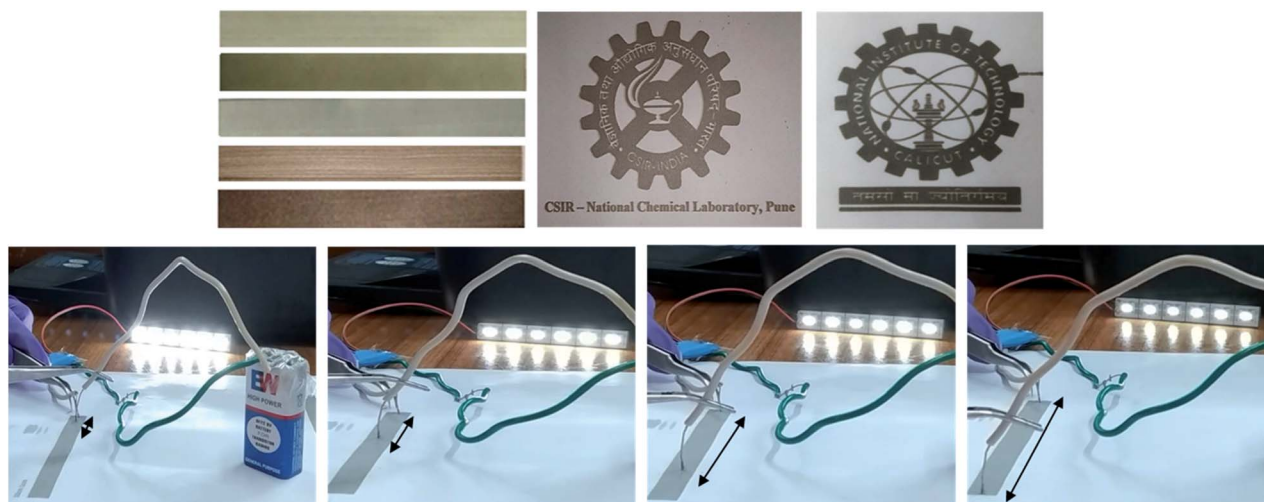


Fig. 7 (Top row) (left) Conductive patterns of AgNW lines at different concentrations (10 mg mL^{-1} , 20 mg mL^{-1} , 30 mg mL^{-1} , 40 mg mL^{-1} , and 50 mg mL^{-1} from top to bottom) and (middle and right) logos of CSIR and NITC printed on an A4 sheet of printing paper; (bottom row) verification of conducting tracks for lighting of LEDs and the effect of the distance between the contact points on the intensity.

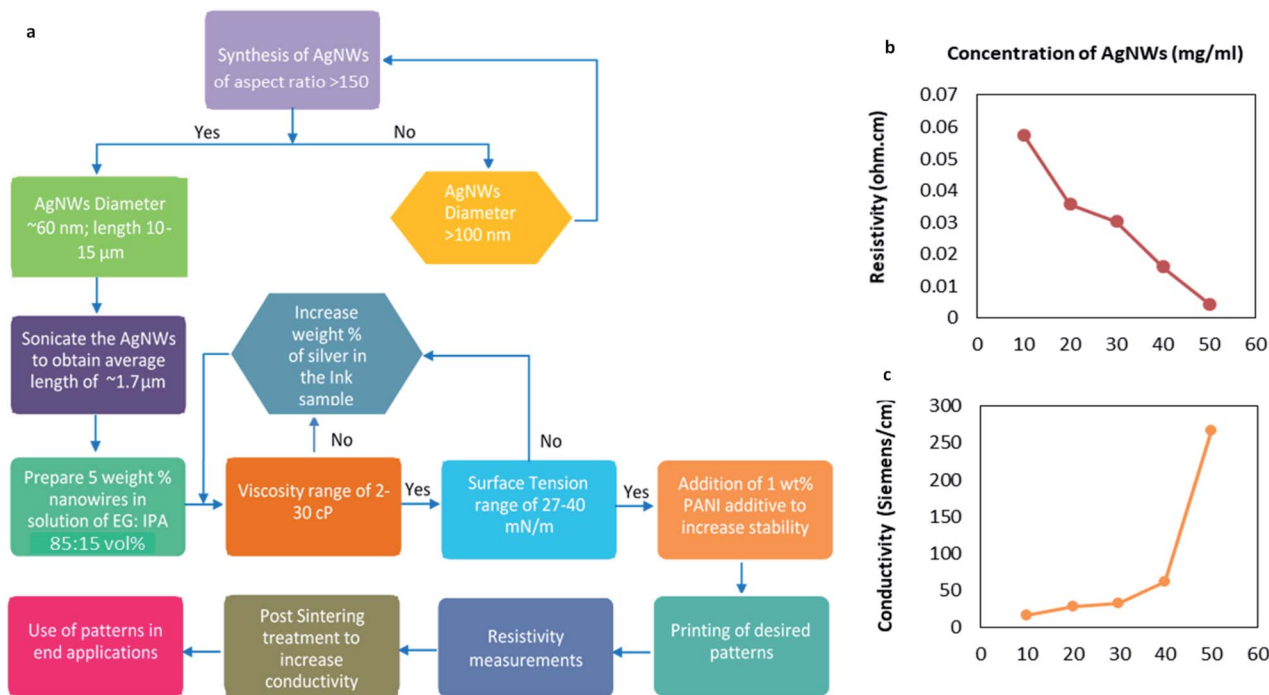


Fig. 8 (a) Flowchart representing the procedure for printing of silver nanowire conducting inks and the effect of the AgNW concentration on (b) resistivity and (c) conductivity.

treatment. For example, one could obtain highly conductive samples ($\sim 6 \Omega \text{ sq}^{-1}$ resistance) within 35 minutes of treatment by either increasing the temperature above 225°C or by keeping lower temperatures at the expense of prolonged treatment times of 60 minutes ($\sim 15 \Omega \text{ sq}^{-1}$ at 210°C). But in view of the time required to reach lower values, it was felt that heating the sample at 300°C for only 10 min would still be a better choice.

Capillary force induced nano-welding. This method is based on a capillary force, and is free of any additional chemical reagents or heating.⁸ It is carried out by simply trapping of water vapour at the junctions of AgNWs by holding a sample inverted on water vapour to condense water droplets on coated nanowire patterns. After drying the samples at room temperature, as shown in the SEM image (inset Fig. 6), the nanowires bend on their surface, due to capillary induced force which improves the conductivity as well as mechanical flexibility. The electrical resistance of these spin coated samples was measured for numbers of cycles of the moisture treatment and is exhibited in Fig. 6. For the first two cycles, resistance reduced very quickly from $2266 \Omega \text{ sq}^{-1}$ to $465 \Omega \text{ sq}^{-1}$ and then reduced very slowly to $71 \Omega \text{ sq}^{-1}$ having a resistivity of $8.023 \times 10^{-3} \Omega \text{ cm}$. Fig. 7 displays different patterns ($10 \text{ mm} \times 100 \text{ mm}$) and printing of the logo of our institutes CSIR and NITC printed on A4 size paper with a AgNW concentration of 50 mg mL^{-1} and optimized nanowire length $\sim 1.72 \mu\text{m}$ and a diameter of $\sim 60 \text{ nm}$. Both the logos were conducting even under bent conditions. The series of images in the second row demonstrate the glowing of LEDs in different intensities with respect to the distance between the contact points. The intensity of light depends on the distance between two contact points. These observations are in accordance with the results obtained by Tobjörk *et al.*²³ The printed

conductive track could be used as an electronic circuit and also applied in other electronic applications.

Electrical measurements. It was found that the thicknesses of patterns in Fig. 7 were varied with the square of the number of passes. The relationship between the thickness and number of passes (N) could be given as [thickness (nm) = $3.16 \times N^{1.95 \pm 0.16}$], which can be used for the estimation of the thickness for a given suspension concentration and using this printer.²¹ The resistance of the sample was calculated as [resistivity = (resistance \times area)/length] and conductivity was obtained as inverse of resistivity. At 10 mg mL^{-1} of the AgNW sample concentration, the pattern displayed a resistance of $763 \Omega \text{ sq}^{-1}$, and the resistivity and conductivity were calculated to be $5.76 \times 10^{-2} \Omega \text{ cm}$ and $17.34 \text{ siemens cm}^{-1}$ respectively. As the concentration of the ink increased, the resistivity decreased and thereby the conductivity increased. The observations are plotted in Fig. 8b and c. At the highest concentration of 50 mg mL^{-1} , the resistivity of ink was lowest ($0.43 \times 10^{-2} \Omega \text{ cm}$) and conductivity increased to $265.96 \text{ siemens cm}^{-1}$. A flowchart that guides one through the procedure for making formulations of highly conductive inks is given in Fig. 8a. We have followed this approach many times and have got perfectly reproducible results. The patterns printed on paper shown in Fig. 8 are found to be conducting even after several months.

Conclusions

Printing of conducting tracks on regular A4 size paper using a commercially available inkjet printer having silver nanowire ink is demonstrated with a highly reproducible protocol. Continuous and smooth lines of a conducting pattern are achieved in 12 passes and the tracks are conductive even after several

months after printing. Printing was achieved using nanowires of 1.72 μm length and a diameter of ~ 60 nm. The nanowires are synthesized by chemical reduction with polyol and dispersed in a simple co-solvent system made of ethylene glycol and isopropyl alcohol to get a conductive ink with a mere 5 wt% concentration of Ag. Importantly, unlike most of the literature that involves transfer of conducting nanowires into other solvents, here we have used AgNWs synthesized directly in EG as it is to make ink formulations. This approach has helped us ensure no loss of this exotic material without compromising on the quality of conducting patterns or their printability. A systematic and reproducible work flow was evolved for making Ag NW inks that can be used for printing conducting tracks. A wire diameter < 70 nm and very short lengths corresponding to ~ 1.8 μm avoid clogging of the cartridge nozzles and ensure a smooth printing process. Nanowire segments of smaller lengths can flow through the nozzles but need significantly higher loading.

Many literature reports mention the use of silver nanoparticle inks with a higher Ag concentration ranging from 15–40 wt%.^{13,44–46} Although commercially available inks require only one pass, using a higher amount of silver will be significantly expensive, since the cost of nano-silver itself will outweigh the cost of the whole printing operation. Using AgNW ink is practical because it is economically feasible to give a greater number of passes (12 in our case) compared to increasing the nano-silver concentration in the ink. It also needs to be realized that the sintering of nanoparticles or nanowires is essential during their printing. Using nanoparticles indeed needs a high loading to avoid breaks in the printed paths, which can be avoided by using a low loading of silver nanowires. Inks made using silver nanowires require a very low concentration of AgNWs and perform very well, thus proving their commercial use in many electronic applications.

The stability of AgNW inks as well as the overall conductivity can be increased by addition of very small quantities of additives such as polyaniline PANI (1%). A post-treatment of sintering of the conductive patterns reduces the resistance (< 100 Ω) and sintering carried out on a spin coated sample (300 $^{\circ}\text{C}$ for 10 min) showed a very low electrical resistance of 2.63×10^{-4} Ω cm after 60 minutes of continuing the treatment (from initial value of 4.7×10^{-3} Ω cm). An alternate to the heat treatment, capillary force induced nano-welding at room temperature is found to improve the conductivity without applying heat, which was carried out by giving moisture treatment, and can be the best treatment for heat sensitive substrates. The resistance of samples reduced from 465 Ω sq $^{-1}$ (in the first two cycles) to as low as 71 Ω sq $^{-1}$ (resistivity of 8.023×10^{-3} Ω cm) after 6 times of moisture treatment.

Conflicts of interest

There are no conflicts to declare.

Acknowledgements

The authors acknowledge the funding from DST (GoI) Advanced Manufacturing Technologies Scheme. Prathamesh Patil thanks

the Chemical Engineering Department of NIT Kozhikode for allowing him to do his MTech project at NCL.

Notes and references

- 1 N. Espinosa, R. R. Søndergaard, M. Jørgensen and F. C. Krebs, *ChemSusChem*, 2016, **9**, 893–899.
- 2 S. J. Choi, S. J. Kim, J. S. Jang, J. H. Lee and I. D. Kim, *Small*, 2016, **12**, 5826–5835.
- 3 J. Vaithilingam, M. Simonelli, E. Saleh, N. Senin, R. D. Wildman, R. J. M. Hague, R. K. Leach and C. J. Tuck, *ACS Appl. Mater. Interfaces*, 2017, **9**, 6560–6570.
- 4 D. Bellet, M. Lagrange, T. Sanniccolo, S. Aghazadehchors, V. H. Nguyen, D. P. Langley, D. Muñoz-Rojas, C. Jiménez, Y. Bréchet and N. D. Nguyen, *Materials*, 2017, **10**(6), 1–16.
- 5 C. Mayousse, C. Celle, E. Moreau, J. F. Manguet, A. Carella and J. P. Simonato, *Nanotechnology*, 2013, **24**(21), 215501.
- 6 H. Lee, M. Kim, I. Kim and H. Lee, *Adv. Mater.*, 2016, **28**, 4541–4548.
- 7 Y. Liu, J. Zhang, H. Gao, Y. Wang, Q. Liu, S. Huang, C. F. Guo and Z. Ren, *Nano Lett.*, 2017, **17**, 1090–1096.
- 8 N. X. Williams, S. Noyce, J. A. Cardenas, M. Catenacci, B. J. Wiley and A. D. Franklin, *Nanoscale*, 2019, **11**, 14294–14302.
- 9 P. Zhang, I. Wyman, J. Hu, S. Lin, Z. Zhong, Y. Tu, Z. Huang and Y. Wei, *Mater. Sci. Eng., B*, 2017, **223**, 1–23.
- 10 Y. Liu, X. Yang, L. Yue, W. Li, W. Gan and K. Chen, *Polym. Compos.*, 2019, **40**, 4390–4401.
- 11 Y. Sun, *Nanoscale*, 2010, **2**, 1626–1642.
- 12 J. Kwon, Y. D. Suh, J. Lee, P. Lee, S. Han, S. Hong, J. Yeo, H. Lee and S. H. Ko, *J. Mater. Chem. C*, 2018, **6**, 7445–7461.
- 13 L. Cao, X. Bai, Z. Lin, P. Zhang, S. Deng, X. Du and W. Li, *Materials*, 2017, **10**(9), 1–9.
- 14 S.-H. Tseng, L.-M. Lyu, K.-Y. Hsiao, W.-H. Ho and M.-Y. Lu, *Chem. Commun.*, 2020, **56**(42), 5569–5706.
- 15 J. Sun, W. Zhou, H. Yang, X. Zhen, L. Ma, D. Williams, X. Sun and M. F. Lang, *Chem. Commun.*, 2018, **54**, 4923–4926.
- 16 S. Fahad, H. Yu, L. Wang, A. Nazir, R. S. Ullah, K. ur R. Naveed, T. Elshaarani, B. U. Amin, A. Khan and S. Mehmood, *J. Mater. Sci.: Mater. Electron.*, 2019, **30**, 12876–12887.
- 17 W. R. De Araujo and W. R. Paixão, *Analyst*, 2014, **139**, 2742–2747.
- 18 H. H. Lee, K. Sen Chou and K. C. Huang, *Nanotechnology*, 2005, **16**, 2436–2441.
- 19 N. C. Raut and K. Al-Shamery, *J. Mater. Chem. C*, 2018, **6**, 1618–1641.
- 20 Z. Liu, Y. Su and K. Varahramyan, *Thin Solid Films*, 2005, **478**, 275–279.
- 21 D. J. Finn, M. Lotya and J. N. Coleman, *ACS Appl. Mater. Interfaces*, 2015, **7**, 9254–9261.
- 22 W. Zhou, F. A. List, C. E. Duty and S. S. Babu, *Metall. Mater. Trans. B*, 2015, **46**, 1542–1547.
- 23 D. Tobjörk, H. Aarnio, P. Pulkkinen, R. Bollström, A. Määttänen, P. Ihalainen, T. Mäkelä, J. Peltonen, M. Toivakka, H. Tenhu and R. Österbacka, *Thin Solid Films*, 2012, **520**, 2949–2955.

- 24 E. Hrehorova, M. Rebros, A. Pekarovicova, B. Bazuin, A. Ranganathan, S. Garner, G. Merz, J. Tosch and R. Boudreau, *IEEE/OSA J. Disp. Technol.*, 2011, **7**, 318–324.
- 25 A. Russo, B. Y. Ahn, J. J. Adams, E. B. Duoss, J. T. Bernhard and J. A. Lewis, *Adv. Mater.*, 2011, **23**, 3426–3430.
- 26 R. Z. Li, A. Hu, T. Zhang and K. D. Oakes, *ACS Appl. Mater. Interfaces*, 2014, **6**, 21721–21729.
- 27 N. M. Abbasi, H. Yu, L. Wang, Z. Abdin, W. A. Amer, M. Akram, H. Khalid, Y. Chen, M. Saleem, R. Sun and J. Shan, *Mater. Chem. Phys.*, 2015, **166**, 1–15.
- 28 Y. Sun, Y. Yin, B. T. Mayers, T. Herricks and Y. Xia, *Chem. Mater.*, 2002, **14**, 4736–4745.
- 29 M. Tsuji, Y. Nishizawa, K. Matsumoto, M. Kubokawa, N. Miyamae and T. Tsuji, *Mater. Lett.*, 2006, **60**, 834–838.
- 30 Y. Li, S. Guo, H. Yang, Y. Chao, S. Jiang and C. Wang, *RSC Adv.*, 2018, **8**, 8057–8063.
- 31 X. Jiang, Y. Xie, J. Lu, L. Zhu, W. He and Y. Qian, *J. Mater. Chem.*, 2001, **11**, 1775–1777.
- 32 Y. Zhou, S. H. Yu, C. Y. Wang, X. G. Li, Y. R. Zhu and Z. Y. Chen, *Adv. Mater.*, 1999, **11**, 850–852.
- 33 S. Coskun, B. Aksoy and H. E. Unalan, *Cryst. Growth Des.*, 2011, **11**, 4963–4969.
- 34 A. Nekahi, S. P. H. Marashi and D. H. Fatmesari, *Mater. Chem. Phys.*, 2016, **184**, 130–137.
- 35 X. Yang, D. Du, Y. Wang and Y. Zhao, *Micromachines*, 2018, **10**, 1–10.
- 36 M. Hummelgård, R. Zhang, H. E. Nilsson and H. Olin, *PLoS One*, 2011, **6**, 1–6.
- 37 Z. Wang, W. Wang, Z. Jiang and D. Yu, *Prog. Org. Coat.*, 2016, **101**, 604–611.
- 38 A. Kamyshny and S. Magdassi, *Small*, 2014, **10**, 3515–3535.
- 39 Y. Hu, Z. Lao, B. P. Cumming, D. Wu, J. Li, H. Liang, J. Chu, W. Huang and M. Gu, *Proc. Natl. Acad. Sci. U. S. A.*, 2015, **112**, 1–6.
- 40 C. Dispenza, M. A. Sabatino, D. Chmielewska, C. Lopresti and G. Battaglia, *React. Funct. Polym.*, 2012, **72**(3), 185–197.
- 41 Z. A. Hu, Y. L. Xie, Y. X. Wang, L. P. Mo, Y. Y. Yang and Z. Y. Zhang, *Mater. Chem. Phys.*, 2009, **114**(2–3), 990–995.
- 42 S. Poyraz, I. Cerkez, T. S. Huang, Z. Liu, L. Kang, J. Luo and X. Zhang, *ACS Appl. Mater. Interfaces*, 2014, **6**(22), 20025–20034.
- 43 J. Coates, Interpretation of Infrared Spectra, A Practical Approach, in *Encyclopedia of Analytical Chemistry*, ed. R. A. Meyers, John Wiley & Sons Ltd, Chichester, UK, 2000, pp. 10815–10837.
- 44 M. Arunakumari, A. G. Mayes and M. S. Alexander, *Materials*, 2019, 1–10.
- 45 E. Balliu, H. Andersson, M. Engholm, T. Öhlund, H. E. Nilsson and H. Olin, *Sci. Rep.*, 2018, **8**, 2–10.
- 46 I. J. Fernandes, A. F. Aroche, A. Schuck, P. Lamberty, C. R. Peter, W. Hasenkamp and T. L. A. C. Rocha, *Sci. Rep.*, 2020, **10**, 1–11.